SAND2019-9000C

THREE-DIMENSIONAL MODEL OF THE SATURN ACCELERATOR WATER TRI-PLATE TRANSMISSION LINE CONNECTION TO THE VACUUM INSULATOR STACK*

K. Struve[ξ] and B. Ulmen

Sandia National Laboratories[η], PO Box 5800, Mail Stop MS 1173
Albuquerque, NM, 87185-1173, USA

Abstract

Calculation of the power flow from the 36 pulse forming lines to the vacuum region of Saturn has always been complicated by the three-dimensional structure of the rod and bottle connections to the vacuum insulator stack. Recently we have completed a 3-D calculation of the bottle configuration and found a large error in previous impedance estimates. We have used this calculation to determine impedance and to construct a 2-D model of each of the 36 bottles of each level of the insulator using the Transmission Line Matrix (TLM) technique. These TLM models are then used in a 2-D model for each of the three levels of the insulator. Each model starts at a measured forward-going pulse in the water tri-plate and ends at the Brehmstrahlung load at the center of the machine. Because of long transmission line lengths and short pulse lengths, each level can be considered independent of the others. A combination of the three models then represents a quasi-3-D model of the load region of the machine. The results of these calculations agree well with measurement and thereby provide confidence in simulation predictions for those areas where measurements are not possible. Details of the 3-D bottle calculation, the TLM model, and results of the load region simulations using this model are given.

I. INTRODUCTION

Saturn is a 30-year-old pulsed power accelerator that is normally used with a three-concentric-ring diode configuration to produce a large-diameter soft x-ray dose for component verification [1]. Nominal peak current and pulse width are 10 MA and 40 ns, with a load voltage of about 1 MV. It consists of 36 parallel pulse generation and forming lines that drive three cathodes of six conical magnetically-insulated transmission lines (MITLs) in vacuum to three independent radiation loads. A diagram of one line is shown in fig. 1. Details of the load can be found elsewhere [2, 3]. A key feature of the design is that the output of each pulse-forming line can be directed to any of the three cathode levels, thus providing flexibility in distribution of the power pulse to the load. Typically, with the three-ring diode configuration, the lower output of each water tri-plate line is connected to the lower cathode. For twenty-four of the lines the upper tri-plate output is connected to the middle cathode, and the remaining twelve are connected to the upper cathode. However circuit modeling of these connections is complicated by the three-dimensional (3-D) geometry of these, which is the subject of this paper.

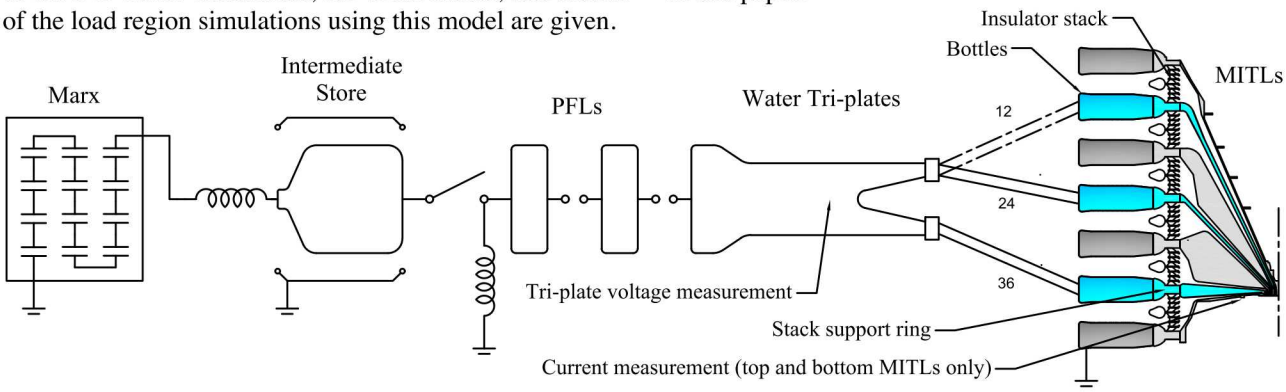

Figure 1. Block diagram of the Saturn pulsed power configuration, one of thirty-six parallel lines showing only the inner conductors of the PFLs and water tri-plate transmission lines.

* Work supported by the US National Nuclear Security Administration under contract DE-NA0003525.

[ξ] email: kwstruv@sandia.gov

[η] Sandia National Laboratories is a multi-mission laboratory managed and operated by National Technology and Engineering Solutions of Sandia LLC, a wholly owned subsidiary of Honeywell International Inc.

II. Tri-Plate to Vacuum Connections

Connections from the water tri-plate transmission lines are made with 8-Ω rods that attach to cylindrical bottles that are bolted to support rings of the vacuum insulator stack. The top-down view in fig. 2 shows that the rod connects between two adjacent bottles. Here rods can be seen connected to cathodes of two levels. For clarity the anode connections are retracted. Note that there are thirty-six bottles on each of the seven levels (four anode and three cathode), for a total of 252 bottles. Each is 673 mm long and diameter 229 mm, as shown in fig. 3. With $\varepsilon_r = 81$ for water, its electrical length is 20.2 ns.

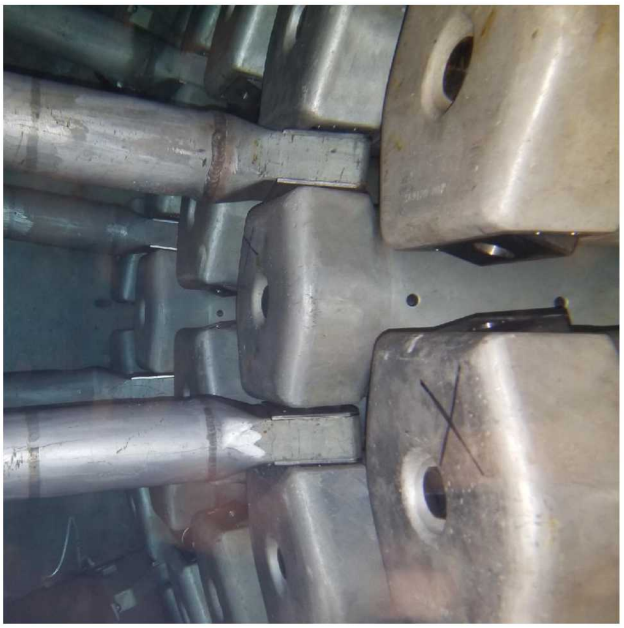

Figure 2. Rod-to-bottle cathode connections.

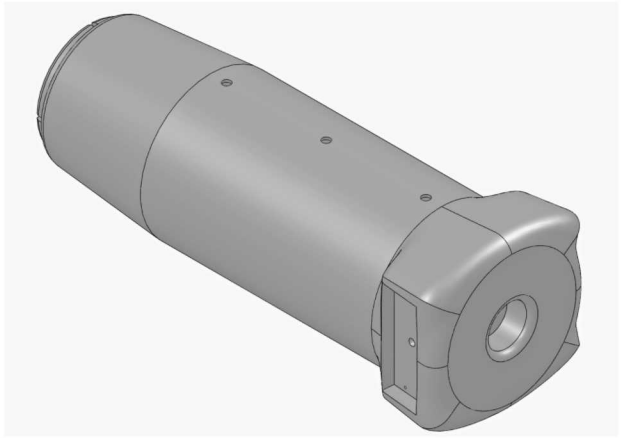

Figure 3. CAD model of one bottle.

A. *Bottle Connection Impedance*

The impedance of the rod-to-bottle connection is determined with a 3-D electrostatic code calculation. This geometry was redrawn within the Coulomb code [4] maintaining the gross dimensions but leaving out holes and other minor details. This model was then replicated 108 times to represent one cathode level and its two adjacent anode levels as shown in fig. 4. The calculation yields a capacitance of 56.3 nF between the middle cathode row, and the upper and lower anode rows. Thus its impedance is 20.2 ns / 56.3 nF = 0.359 Ω, or 12.9 Ω for one bottle, which is 30% lower than previously used [5].

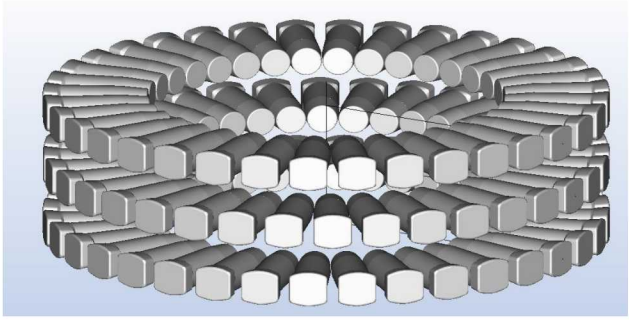

Figure 4. Coulomb code model of one cathode level of the bottle-to-insulator stack connection.

B. *Two-Dimensional Representation of the Bottle*

The 2-D connection of the rods to the bottles leads to representing each bottle as a 2-D transmission-line-matrix (TLM) block [6] for circuit modeling. A schematic is shown in fig. 5. This configuration consists of interconnected short transmission line elements that allow both axial and transverse power flow. A key requirement is that the length of each element must be a small fraction of the rise-time of the pulse, which they are. The values of the individual components are adjusted to match the bottle capacitance and to give correct propagation delay. Also the rectangular grid propagation lengths must be adjusted by a factor square-root of two to accommodate diagonal current paths. With this technique it is possible to drive the bottle from one or two sides, or to have it stand alone as a capacitive load when not connected to a rod.

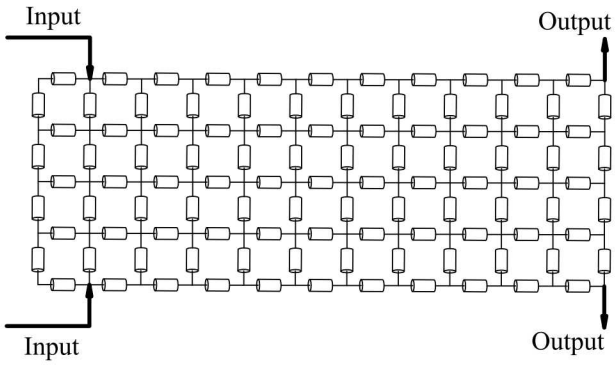

Figure 5. TLM model of bottle. Each transmission line element is 86.3 Ω and 1.43 ns long.

III. 2-D CIRCUIT MODEL

It has recently become important to determine the voltage at the insulator stack as we upgrade the accelerator. That voltage is currently not measured. Voltage measurements have been made in the bottle region but are suspect and likely not representative of the voltage at the stack. Therefore the approach for the latest modeling is to start with the measured voltage in the water tri-plate transmission lines, and compare circuit-code predictions to current measurements in the vacuum MITLs. We are limited however to measurements in two of the six MITLs, those that are most accessible. If we start with a measured voltage and closely match measured currents in the MITLs, the circuit-code generated stack voltages should be fairly accurate. For these simulations we use the Bertha code [7], a transmission line code that models individual components as transmission line elements.

A. Circuit Model Setup

Because the three diodes are not connected at the center of the machine and because the roundtrip time between their common connection in the water tri-plate is much longer than the 40-ns pulse length, the circuit can be split into three independent 2-D models. These models are the lower cathode, the A and B MITLs; the middle cathode, the C and D MITLs; and the upper cathode, the E and F MITLs. Together these represent a quasi-3-D model of the machine. Each is driven by the same number of equivalent voltages as the number of rods attached to that level.

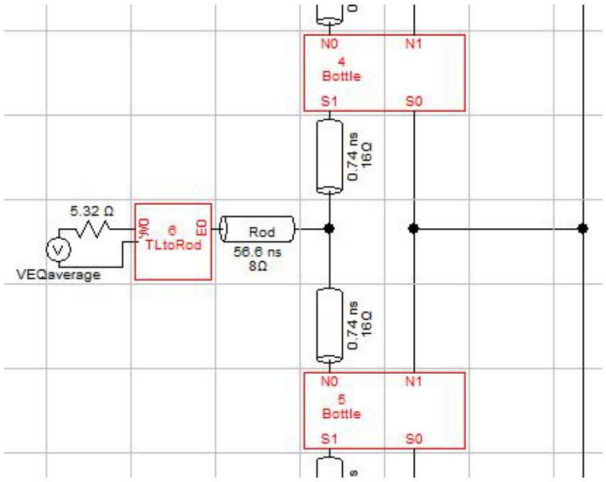

Figure 6. Drive circuit for one rod and two bottles.

The circuit that drives one rod and two bottles is shown in fig. 6. Its Bottle block is as shown in fig. 5, and its TLtoRod block contains transmission line elements for the tri-plates. The drive voltage is shown in fig. 7. This circuit is connected in parallel with its adjacent lines to simulate drive lines coming in at all azimuths to the vacuum stack. The upper side of topmost block in the schematic is connected back to the lower side of the lowest. Currently we are using an average of all the measured tri-plate voltages as the drive voltage. But we intend to also use individual line signals to investigate effects of timing spread and voltage variations.

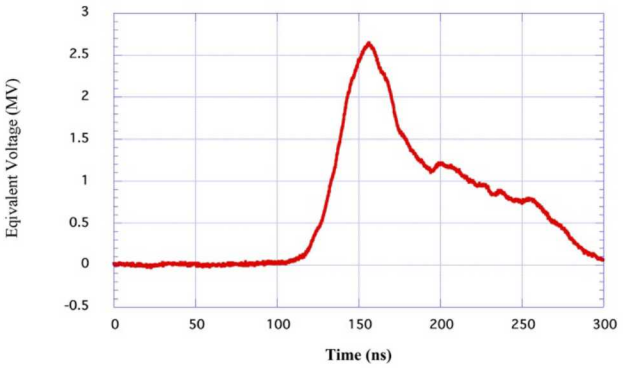

Figure 7. Equivalent drive voltage which is an average of twice the measured voltage of each of the 36 lines.

After this parallel connection at the vacuum stack the circuit transitions back to a 1-D model. That is feasible since transmission times are much shorter in the vacuum MITLs. An improvement would be to extend the 2-D structure into the vacuum section with the TLM approach.

The short water transmission line from the bottle connection to the stack support-ring, the insulator stack, and the vacuum transmission lines to the diode are all modeled separately for each of the six MITLs. Each consist of many 0.1 ns long transmission line elements with impedances determined from the stack and MITL drawings. Also, the constant impedance section of the MITL to the load is modeled as a lossy MITL using the MITL model in Bertha. This model inserts Child-Langmuir emission loss before magnetic insulation is established. Each pair of MITLs is connected at the diode, which is modeled in Bertha with its Ring-Diode model. Parameters are chosen to be consistent with diode dimensions and expected gap closure velocities.

B. Simulation Results

Comparison of the model's MITL-current predictions with measured currents for Saturn shot 4425 are shown in figs. 8 and 9. The colored lines are the data, and the black lines the simulations. This was a normal three-ring diode shot with current measurements at three azimuths near the diode on the lowest MITL (level A) and the highest MITL (level F). For this shot 36 rods were connected to the AB (lower) cathode, and 12 to the EF (upper) cathode.

The A-MITL current measurements were not consistent, indicating possible diagnostic problems. But the simulated current sits between the high and low measurements. The simulation of the F-MITL current matches the measurements fairly well. The discrepancy after peak current may be related to uncertainty in use of the diode model. Adding the currents of the other MITLs (not shown) yields a total peak diode current of 9.0 MA.

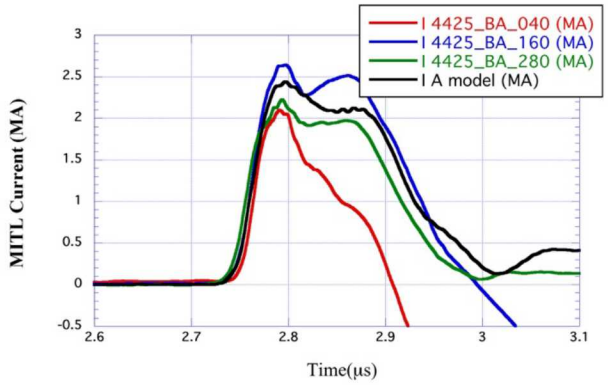

Figure 8. A MITL current measurement and prediction.

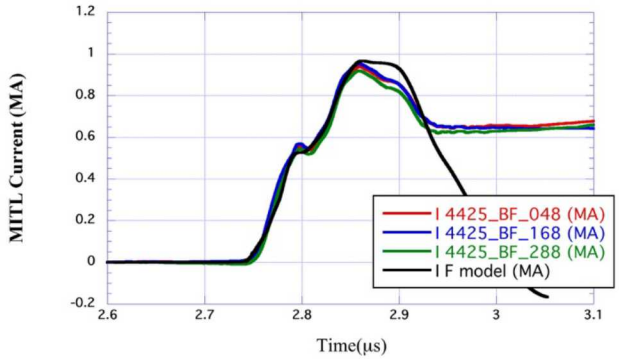

Figure 9. F MITL current measurement and prediction.

Predicted stack voltage from the simulation for this shot is shown in fig. 10. Here peak voltage of the AB stack is 2.4 MV, 2.3 MV on the CD stack, and 1.5 MV on the EF stack. The voltage on EF is lower because it is powered by fewer rods, has unpowered bottles attached, and has the highest inductance MITLs. Since each stack height is 30.5 cm, peak fields on the AB, CD, and EF stacks are 79, 75, and 49 kV/cm, respectively.

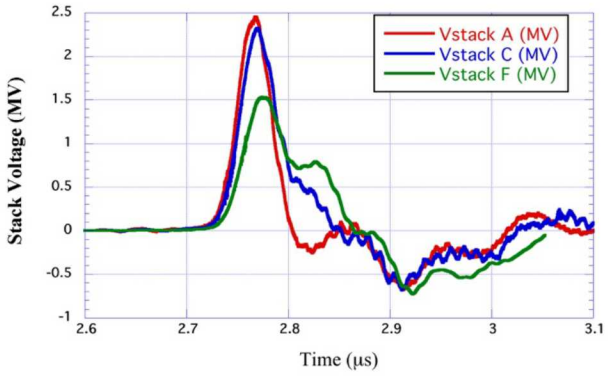

Figure 10. Code predicted stack voltages

IV. SUMMARY

We have been able to successfully characterize and model the load region of Saturn. We have determined the impedance of the bottle connection with a 3-D electrostatic calculation. We have modeled the bottles as 2-D transmission line matrices to better handle non-uniform connection geometries. We have developed three independent 2-D models, one for each of the three rings of the diode. We have used these models to successfully match measured currents near the diode. Thereby we have determined peak voltages at the stack, a measurement that is now not practical on Saturn. These predictions indicate that peak fields on the stacks are very conservative. Thus it is possible to reduce load region inductance and thereby allow yet higher current and diode yields. We also now have a tool to investigate the effects of timing spread and voltage variations from line to line on diode behavior.

V. REFERENCES

[1] D. D. Bloomquist, R. W. Stinnett, D. H. McDaniel, J. R. Lee, A. W. Sharpe, J. A. Halbleib, L. G. Schlitt, P. W. Spence, and P. Corcoran, "Saturn, A Large Area X-ray Simulation Accelerator," *Proc. of the Sixth IEEE Pulsed Power Conf.,* Arlington, VA edited by P. J. Turchi and B. H. Bernstein (IEEE, New York, 1987), p. 310.

[2] M. A. Hedemann, J. R. Lee, J. A. Halbleib, G. A. Carlson, G. T. Baldwin, W. A. Stygar, R. J. Leeper, D. L. Fehl, A. W. Sharpe, and L. M. Choate, "Characterization of the Saturn Bremsstrahlung Source," *Proc. of the Sixth IEEE Pulsed Power Conf.,* Arlington, VA edited by P. J. Turchi and B. H. Bernstein (IEEE, New York, 1987).

[3] K. W. Struve, T. C. Grabowski, N. R. Joseph, B. V. Oliver, M. E. Savage, B. A. Ulmen, and P. J. Vandevender, "Estimates of Saturn Radiation Output Scaling versus Machine Design Parameters" in Proc. of the 2018 Int. Conf. on Megagauss Magnetic Field Generation and Related Topics, ieeexplore.ieee.org, p. 63.

[4] Coulomb, a 3-D electrostatic Green's functions Laplace equation solver by Integrated Engineering Software, Winnipeg, Canada.

[5] P. Corcoran, L. Schlitt, P. Spence, and G. Proulx, "Saturn Electrical Design Final Report," PSI-FR-208, July 1986, Pulse Sciences Inc., 14796 Wicks Blvd., San Leandro, CA 94577.

[6] C. Christopoulos, *The Transmission Line Modeling Method: TLM*, Piscataway, NY, IEEE Press, 1995.

[7] Bertha transmission-line circuit code, D. Hinshelwood, U. S. Naval Research Laboratory, Washington, DC.